



Published in final edited form as:

Osteoporos Int. 2010 June ; 21(6): 985–995. doi:10.1007/s00198-009-1044-5.

Longitudinal changes in femur bone mineral density after spinal cord injury: effects of slice placement and peel method

S. Dudley-Javoroski and R. K. Shields

Graduate Program in Physical Therapy and Rehabilitation Science, The University of Iowa, 1-252 Medical Education Building, Iowa City, IA 52242-1190, USA

R. K. Shields: richard-shields@uiowa.edu

Abstract

Summary—Surveillance of femur metaphysis bone mineral density (BMD) decline after spinal cord injury (SCI) may be subject to slice placement error of 2.5%. Adaptations to anti-osteoporosis measures should exceed this potential source of error. Image analysis parameters likewise affect BMD output and should be selected strategically in longitudinal studies.

Introduction—Understanding the longitudinal changes in bone mineral density (BMD) after spinal cord injury (SCI) is important when assessing new interventions. We determined the longitudinal effect of SCI on BMD of the femur metaphysis. To facilitate interpretation of longitudinal outcomes, we (1) determined the BMD difference associated with erroneous peripheral quantitative computed tomography (pQCT) slice placement, and (2) determined the effect of operator-selected pQCT peel algorithms on BMD.

Methods—pQCT images were obtained from the femur metaphysis (12% of length from distal end) of adult subjects with and without SCI. Slice placement errors were simulated at 3 mm intervals and were processed in two ways (threshold-based vs. concentric peel).

Results—BMD demonstrated a rapid decline over 2 years post-injury. BMD differences attributable to operator-selected peel methods were large (17.3% for subjects with SCI).

Conclusions—Femur metaphysis BMD declines after SCI in a manner similar to other anatomic sites. Concentric (percentage-based) peel methods may be most appropriate when special sensitivity is required to detect BMD adaptations. Threshold-based methods may be more appropriate when asymmetric adaptations are observed.

Keywords

Bone mineral density; Femur; Longitudinal; pQCT; Spinal cord injury

Introduction

Following spinal cord injury (SCI), disruption of normal neural, vascular, hormonal, and mechanical factors precipitates rapid bone loss in paralyzed extremities. Recent studies employing peripheral quantitative computed tomography (pQCT) have revealed that adaptations to SCI differ both quantitatively and qualitatively among different anatomic regions of long bones. Trabecular bone mineral density (BMD) of the distal femur epiphysis declines by as much as 54% in the first 4 years post-SCI, after which BMD reaches a relative

Correspondence to: R. K. Shields, richard-shields@uiowa.edu.

Conflicts of interest None.

steady state [1]. This decline in trabecular BMD reflects degradation of trabecular architectural elements over time post-SCI [2]. In contrast, femur diaphysis cortical BMD remains stable or only minimally declines after SCI [1,3]. The primary adaptation to SCI at diaphyseal sites is resorption of cortical bone at the endosteal surface [4], causing cortical wall thickness to decline by as much as 47% [1,4]. As a consequence of these deleterious adaptations, the lifetime fracture risk for people with SCI is double the risk for the non-SCI population [5]. Moreover, the hazard for mortality is estimated to be 78% higher for people with SCI who sustain a lower extremity fracture than their peers without fractures [6].

The femur metaphysis is a transition zone between the condyles (which contain extensive trabecular bone and a thin cortical shell) and the diaphysis, a thick cortical shell with almost no trabecular bone present. Longitudinal post-SCI BMD data are scarce [7–10], but cross-sectional studies suggest that BMD decline at the femur epiphysis occurs more rapidly than at tibial sites [1]. The rapid and extensive loss of bone mineral in the distal femur makes it very prone to fracture, even with small external forces [11]. Along with the femoral condyles, the femur metaphysis is the most common site for fracture after SCI [12,13]. But despite its clinical significance, no previous pQCT studies have quantified BMD at this site. Rittweger and colleagues reported bone mineral content, rather than density for this region [14], while Eser and colleagues reported BMD for the epiphysis [1]. Non-SCI normative values and longitudinal subacute SCI values currently are not available in the literature.

The external contour of the femur narrows rapidly in the metaphyseal region. In addition, the marrow cavity begins to form, becoming wider and more distinct in the proximal regions of the metaphysis. These sources of contour variation affect the amount of trabecular bone that is present in any particular pQCT image of the femur metaphysis. Because the trabecular anatomy of the metaphysis changes rapidly from distal to proximal, trabecular BMD (the mean density of the trabecular envelope) may be similarly variable. If this is the case, slice placement errors during pQCT scans of the transition zones such as the femur metaphysis could lead to erroneous BMD values. Particularly during longitudinal studies, slice placement errors become an important factor that may influence accurate bone density assessment.

Our laboratory has previously examined the effect of slice placement errors at the tibia distal epiphysis. When slices were intentionally misplaced 3 mm from the true 4% tibia site (measured from the distal end), BMD differences were as high as 5% [15]. We suggested that ideal anti-osteoporosis interventions should yield an effect size greater than 5% in order to exceed this potential source of error. However, the 4% tibia site lies distal to the formation zone for the tibia marrow cavity. In addition, the external contour of the distal tibia changes less dramatically than the external contours of the distal femur. Accordingly, BMD differences due to slice misplacement in the femur metaphysis may be greater than those obtained from the tibia. Additionally, our previous study of the distal tibia 4% site revealed that BMD differences due to slice misplacement were twice as high (4.6%) for subjects with SCI than for subjects without SCI (2.3%).

Another unresolved issue with pQCT assessment of the femur metaphysis is whether image processing should include a concentric “peel” step. In several previous studies of the tibia and femur epiphyses, investigators applied an algorithm to concentrically peel away rows of voxels, regardless of density, starting at the periosteal surface [1,16]. This process eliminates all but the central core (usually 45%) of the image from BMD analysis. While this strategy ensures that no voxels containing cortical bone enter the analysis, it also eliminates a substantial portion of the trabecular voxels at the periphery of the bone cross-section. Because destruction of trabecular elements may be most severe in the central region of the tibia epiphysis cross-section [15], application of a concentric peel may force the analysis to consider only a fraction of the available surviving trabeculae. In bone regions with (1) preferential post-SCI loss of central

trabeculae, like the distal tibia, or (2) a nascent marrow cavity, like the femur metaphysis, BMD output may be strongly affected by the use of a concentric peel. Additionally, if the influence of peel method on BMD differs in high- versus low-density images, peel method may have important ramifications during the longitudinal assessment of BMD after SCI.

The purpose of this study is to determine the longitudinal effect of SCI on bone mineral density of the femur metaphysis. We will (1) determine the BMD difference associated with erroneous slice placement, in comparison to the previously determined tibia value; (2) determine the effect of operator-selected peel algorithms on BMD; and (3) compare SCI and non-SCI BMD values for the femur metaphysis site longitudinally.

Methods

Subjects

Fifteen individuals (one female) with SCI (ASIA A and B [17]) participated in the study. Time post-SCI at the first pQCT date ranged from 0.19 to 7 years (Table 1). An additional ten healthy adults (one female) without SCI or other musculoskeletal or neurological disorders served as a control cohort. The cohorts did not differ according to age ($p=0.40$) or stature (femur length, $p=0.42$). The protocol was approved by the University of Iowa Human Subjects Institutional Review Board and all subjects provided written informed consent before participating. Exclusion criteria for all subjects were a history of bone pathology (i.e., bone metabolic disease, cancer, etc.), thyroid disorder, previous fracture at the scan site, pregnancy or possible pregnancy, and medications known to affect bone metabolism. Subjects with SCI were excluded if they experienced frequent spasms that would likely induce pQCT scan artifacts. The scan session time for both limbs (including time for transfers and positioning) was approximately 90 min.

This study was conducted as a mixed cross-sectional and longitudinal design. SCI subjects 1–5 (Table 1) were first assessed in the acute post-SCI stage (<4 months). Bilateral pQCT data are available from these subjects, with unilateral data thereafter. SCI subjects 6–15 underwent unilateral testing between one and six times, with each scan separated by at least 3 months. SCI subjects 3, 4, 7, and 9 also participated in passive standing on 3–5 days per week, which could have theoretically led to a small bone-sparing response. This possibility seems remote, however, as previous studies revealed minimal bone-sparing effect of passive standing on femur BMD in subjects with SCI [18,19].

Nine of the non-SCI control subjects underwent one time, bilateral pQCT assessment. The left limb of the tenth control subject (N7, Table 1) was not scanned due to the presence of surgical hardware in the distal femur. We recruited the non-SCI cohort because we desired an estimate of typical non-SCI BMD at this anatomic location, as this information has not been previously reported. Bilateral scans were conducted in order to capture an estimate of within-subject BMD variability between limbs.

Data reduction

Longitudinal data were partitioned into time bins to allow statistical analysis of BMD over time (Fig. 1). The key requirement for bin selection was that no subject should contribute multiple data points to any given bin. (The exception to this is bin 1, which contains bilateral data for subjects with acute SCI. The two limbs are presented separately for bin 1, rather than pooled). The six time bins described in Fig. 1 allowed the maximum data points in the data set to be used (29 of 37), without multiple representation of any subject in a bin.

Scan procedure

pQCT measurements are performed with a Stratec XCT-2000 or 3000 densitometer (Stratec Medical, Pforzheim, Germany). Accuracy of this device is 2% (to the COMAC phantom); precision is ± 3 mg/cm³ for trabecular bone and ± 9 mg/cm³ for cortical bone [20]. Within-subject variation for BMD of the distal femur has been reported to be between 1.80% and 3.80%, depending on the anatomic location [1]. This device is calibrated with respect to fat (fat density=0 mg/cm³).

Femur length was obtained via palpation of the greater trochanter and the lateral femoral condyle by the investigator. After determination of femur length with a measuring tape, the investigator passed the limb through the pQCT gantry and secured the subject's foot onto a footplate. A radiology technician performed a scout view of the tibiofemoral joint and placed a reference line at the distal limit of the lateral femoral condyle. Using this reference line, the scanner obtained an image at 12% of femur length. Voxel edge length was 0.4 mm, scanner speed was 25 mm/s, and slice thickness was 2.2 mm.

Slice placement

We previously determined that pQCT slice placement errors of 3 mm are possible due to extreme instances of mis-measurement of tibia length [15]. BMD errors of up to 5% occurred with intentionally erroneous tibia slice placement at 3 mm intervals. In the present study, we wish to obtain an analogous error estimate for the distal femur. We anticipated that because of the broad shape of the greater trochanter and because it lies beneath copious soft tissue, femur length mis-measurement may be large, causing slice location error to be greater than in the tibia. The investigator measured and remeasured femur length in blinded fashion from six subjects, three with SCI (S4, S13, S14) and three without (N3, N5, N10). Within rater test-retest concordance (ICC 3, 1) [21] was 0.83. The worst-case test-retest difference for any subject was 24 mm. Average femur length for the combined SCI and non-SCI cohorts was 470.72 mm. An image slice at 12% of this length would be obtained at 56.5 mm. If a worst-case mis-measurement of femur length occurred (24 mm), the erroneously obtained femur length would be 494.72 mm. An image slice at 12% of this length would be obtained at 59.4 mm, or 2.9 mm from the actual 12% slice location. This is nearly identical to the 3 mm potential slice misplacement errors we previously estimated for the tibia [15]. For this reason, we used serial scans spaced 3 mm apart to estimate BMD differences due to slice misplacement for the femur metaphysis. We obtained images at 12% of femur length and at 3 mm proximal and 3 mm distal to this point.

Analysis procedures

The investigator defined a region of interest that incorporated a small amount of soft tissue outside of the femur periosteal margin. A threshold algorithm removed voxels below 200 mg/cm³, starting from the outer edge of the region of interest and moving inward. This removed all voxels corresponding to muscle and fat and defined the periosteal edge. Inside the periosteal border, densities higher than 400 mg/cm³ were defined as cortical/subcortical bone and values lower than this threshold were defined as trabecular bone. Cortical/subcortical voxels were excluded from further analysis. A 3 × 3 voxel filter then proofed the remaining image to detect pockets of high-density values. Voxels that had substantially higher BMD than the neighboring voxels were reassigned as subcortical bone and were excluded from further analysis. Trabecular BMD was obtained from the resulting image (a trabecular core with the cortical shell “peeled” away according to density criteria, not a percentage criteria; Fig. 2). Throughout this report, we will refer to this technique as the “threshold peel” method. Because the cortical shell is very thin at the 12% site (and is therefore subject to the partial volume effect [22]), we report only trabecular BMD.

Effect of peel method

Using the analysis method described above, the original image area was peeled away according to threshold criteria, eliminating the cortical shell but preserving all available trabecular envelope voxels for trabecular BMD analysis. In studies of epiphyseal regions, other research groups have instead used a percentage peel technique which concentrically strips away voxels from the periosteal border inward, regardless of the density of these voxels [23,24]. To systematically explore the effect of peel technique on BMD values, we repeated all analyses using a percentage-determined concentric peel algorithm. As above, we delineated the periosteal contour using a 200 mg/cm³ threshold. Next, we applied a concentric peel starting at the periosteal edge and ending when 45% of the original bone area remained (Fig. 2). Trabecular BMD is reported for the preserved trabecular region for the 45% peel method.

Statistical analysis

Group mean and standard error BMD values were calculated for all pQCT slice locations and peel methods. Comparisons between subjects with and without SCI were made using data from the 12% slice and the standard threshold peel technique. A one-way analysis of variance (ANOVA) was used to determine whether BMD for the SCI group is significantly different from the non-SCI group. A repeated measures completely randomized ANOVA was used to establish the effects of slice location (12% slice vs. proximal slice, 12% slice vs. distal slice) for each group. A second repeated measures completely randomized ANOVA was performed to establish the effects of peel method (“threshold peel” method vs. 45% peel) for each group. Significance was set at *P* less than 0.05.

Results

Effect of slice placement

Figure 3 illustrates the outcome of slice misplacement (3 mm) on femur BMD. For the control cohort, mean (SE) BMD at the proximal site (208.3 (6.6) mg/cm³) was significantly lower than the 12% site (*p*<0.05). Average proximal slice BMD was 5.4 mg/cm³ (2.6%) lower than the 12% site. The maximum percent difference (the largest percent difference observed in any subject) between these locations was 11.0% (4.9%). Mean (SE) BMD at the distal site (221.9 (5.8) mg/cm³) was significantly higher than the 12% site (*p*<0.05). Average BMD difference between the distal slice and the 12% site was 4.8 mg/cm³ (2.3%). The maximum percent difference between these locations was 9.3% (4.4%). Thus at 3 mm intervals from the 12% site in the control cohort, BMD declined from distal to proximal and varied across sites by 2.3 and 2.6%. Maximum differences did not exceed 4.9%.

In the SCI subjects, mean (SE) BMD was 158.5 (8.8), 162.2 (8.9), and 165.6 (8.9) mg/cm³ for the proximal, 12%, and distal slices, respectively (Fig. 3). As with the control cohort, BMD at the 12% site was significantly higher than BMD at the proximal site and significantly lower than BMD at the distal site (*p*<0.05). Average proximal slice BMD was 3.7 mg/cm³ (2.4%) lower than the 12% site. The largest percent difference in BMD between these locations was 7.3%. Average BMD difference between the distal slice and the 12% site was 3.4 mg/cm³ (2.3%). The largest percent difference in BMD between these locations was 10.4%. Thus at 3 mm intervals from the 12% site in the SCI cohort, BMD typically varied by 2.3 to 2.4% and maximum differences did not exceed 10.4%.

To summarize, BMD at 3 mm intervals surrounding the 12% femur slice varied to a similar degree in people with and without SCI (*typical BMD errors*=2.3–2.6%). However, maximum percent differences due to slice placement were higher in the SCI group than in the control cohort (10.4% versus 4.9%).

Effect of peel method

Figure 3 (right) depicts the effect of reprocessing the image of the 12% slice using a 45% concentric peel. (For clarity, the distal and proximal slices will not be considered). For the SCI group, application of a 45% peel reduced mean BMD by an average of 17.3% from the “threshold peel” value ($p < 0.05$). The maximum difference from the original BMD with this peel method was 44.9%. The difference between peel methods was likewise significant for the control cohort ($p < 0.05$, Fig. 3). Application of a 45% peel reduced mean BMD by an average of 8.0% from the original value. The maximum difference from the threshold peel BMD was 24.9%.

We were interested to determine whether the effect of applying a concentric peel differed in high-BMD versus low-BMD images. We obtained the percent difference in BMD between the threshold peel and the 45% concentric peel method, and then plotted this difference against the threshold peel BMD. The BMD difference created by applying a 45% peel moderately ($r^2 = 0.640$), negatively correlated with threshold-peeled BMD (Fig. 4). Thus for images with low BMD, application of the 45% concentric peel method yielded large BMD differences from the value obtained with the threshold peel method. For higher density images, BMD differences between the partitioning methods were smaller.

In summary, for subjects with and without SCI, application a 45% peel yielded significant reductions in BMD values when compared to the “threshold peel” method (17.3% and 8.0% respectively.) BMD reductions of 44.9% and 24.9% were possible for these groups. BMD differences between the peel methods were most pronounced in lower density images.

Effect of SCI

Figure 5 depicts all data points from the 12% slice using the threshold peel analysis method. For SCI subjects with bilateral scans in bin 1 and for control subjects, between-limb correlation in BMD was high ($r^2 = 0.99$ and 0.88 , respectively). Mean (SD) control cohort BMD was 213.7 (28.8) mg/cm^3 (range 153.8 to 254.2 mm/cm^3). Standard error of the mean was 6.79 . All SCI BMD values were one standard deviation below the control cohort BMD by 1.5 years post-SCI and two standard deviations below the control value by 2 years. After 2 years post-injury, all but one SCI BMD value fell below the lowest range of control BMD values (< 153.8 mg/cm^3).

Figure 6 illustrates the progression of BMD decline partitioned according to the time bins depicted in Fig. 1. SCI cohort BMD did not differ from control BMD in bin 1 ($p = 0.41$) but was significantly lower than control BMD for all bins thereafter ($p < 0.05$). BMD declined over the first two years post-SCI (bins 1–5) according to a first-order regression equation $y = (-3.93)x + 215.89$, eventually reaching a bin 6 mean/SE value of 84.4 (7.90) mg/cm^3 . This bin 6 BMD was only 39.5% of the non-SCI BMD value.

The small number of subjects with SCI reduces the confidence with which we can calculate a rate of bone loss per month. However, we wished to obtain a preliminary rate estimate for the subjects who were sampled in the first 2 years post injury. We subtracted these 26 SCI data points from the control cohort mean BMD (213.7 mg/cm^3), expressed this difference as a percent of the control BMD, and divided by time post-SCI. In the first 2 years after SCI, subjects lost an average of 1.7% of the projected initial BMD per month (SE: 0.37%).

Four subjects underwent longitudinal testing during bin 6 (Fig. 5). The first and final scans for these subjects were compared to determine whether BMD changed over time for these subjects during the chronic SCI period (> 2 years). The first and final scans were separated by 8 months to 2.2 years. No statistically significant BMD change occurred over time during the course of bin 6 tracking (first vs. final scans $p = 0.75$). Eser and colleagues suggest that the distal femur

may reach a BMD steady state at ~4.1 years post-SCI [1]. Three of the four subjects in bin 6 have exceeded this time point and their BMD trends appear to be in congruence with Eser's findings. These three subjects may demonstrate a steady state BMD plateau, as has been observed in other populations with chronic SCI [1,25].

Discussion

The purpose of this study was to determine the longitudinal effect of SCI on bone mineral density of the femur metaphysis. To correctly interpret longitudinal findings, it is necessary that we estimate sources of error that may affect BMD output values. Thus, along with tracking BMD changes over time post-SCI, our specific objectives were to: (1) determine the BMD difference associated with erroneous slice placement, in comparison to the previously determined tibia value, and; (2) determine the effect of operator-selected peel algorithms on BMD.

Effect of slice placement

In the control cohort, trabecular BMD declined from distal to proximal by 2.3–2.6% over each 3 mm increment. This degree of BMD difference due to slice placement is similar to the errors observed in the SCI cohort (2.3–2.4%). Thus, in most cases, slice misplacement by 3 mm yielded a similar degree of BMD difference in people with and without SCI. However, maximum differences for the SCI group (up to 10.4%) were more than twice as high as the maximum differences for the control group (4.9%).

Due to considerations of radiation dosage and as a matter of convenience, most previous pQCT studies have reported BMD from only one slice per anatomic region. Studies like ours which employ serial slices are less common, particularly in the SCI literature. (Prolonged scan times required for serial slices increase the possibility of involuntary spasms and consequent scan artifacts.) Rauch and coauthors previously noted BMD variation of 8.1% over a 6 mm span in the radius of children without neuromuscular pathology [26]. In the proximal tibia metaphysis of children with cerebral palsy, BMD varied to a much higher extent (16.8% over just 1 mm) [27]. We previously determined that BMD varied by an average of 4.6% over a 3 mm span in the distal tibia epiphysis of adults with chronic SCI [15], higher than the slice placement differences observed in this study of the femur metaphysis (2.3–2.6%).

Although BMD appears to be less variable at the femur metaphysis than the tibia epiphysis for subjects with SCI, 3 mm slice misplacements may or may not be typical in studies of femur BMD. During pilot work, we expected that femur slice-placement errors could be larger than 3 mm because the thick soft tissues over the greater trochanter may complicate femur length measurement. However, we found that within-rater reliability in measuring femur length was acceptable [21] (ICC 0.83). A worst-case instance of femur length mis-measurement (24 mm) would yield a slice placement error of 2.9 mm, very comparable to the 3 mm error margin for the tibia, facilitating comparisons between tibia and femur BMD values.

Our estimate of 3 mm slice misplacement error makes the assumption that no error occurred during placement of the scout view reference line at the distal femur during prescan preparations. Misplacement of the reference line is an independent source of error that may contribute to pQCT slice misplacement. However, reference line errors could either magnify or mitigate slice placement errors due to femur length mis-measurement. That is, a “12%” slice erroneously placed 3 mm too far in the distal direction could be counteracted if the scan operator erroneously placed the scout view reference line 3 mm too far in the proximal direction. Determination of the interaction between these two independent error sources requires a separate reliability study of pQCT reference line placement. However, in practical terms we believe that the 3 mm slice misplacement estimate used in this report may represent the vast

majority of pQCT scan scenarios, because 3 mm error reflected a worst-case limb measurement error. Average slice misplacement due to limb length mis-measurement was only 1.5 mm. It is therefore likely that in many cases, adding reference line misplacement error may still yield a slice placement within the 3-mm range examined in this report. If this is indeed the case, the BMD variability estimates in this report would continue to apply. Future studies should examine the role of scout view reference line placement in pQCT measurements of subjects with SCI.

Because of the difficulty in obtaining femur length, previous groups have considered the femur length to be equal to the tibia length [1]. We do not favor this approach because tibia length has previously been shown to be more variable than femur length [28], and femur length has generally been shown to exceed tibia length [29,30]. It is unclear what effect this approach may have on accurate placement of a slice at a particular percentage of femur length. In cases where femur length exceeds tibia length, a “12%” femur slice would be obtained distal to that individual's actual 12% femur location. Trabecular BMD for that subject may be artificially elevated, per the BMD trends detected in this report.

The present report treats BMD variation due to slice placement in a cross-sectional manner, establishing the percent variation in BMD that may be present at any one measurement point. Future studies should examine the longitudinal changes in BMD variability across time post-SCI. We suspect that as time progresses post-SCI, as less and less of the original bone mineral remains, BMD differences between intentionally misplaced sites may decline.

Effect of peel method

BMD obtained by applying a 45% concentric peel was significantly lower than “threshold peel” BMD for subjects with and without SCI ($p<0.05$). Differences attributable to peel selection were particularly high for the SCI group. BMD with a 45% peel differed from “threshold peel” BMD by only 8.0% in the control group, compared to 17.3% for subjects with SCI. Further examination of pQCT output data revealed the cause of this relative difference. In subjects without SCI, the threshold-based peel method typically allowed 63% of voxels in the region of interest (ROI) to enter the BMD analysis. Peeling this area further inward to 45% yields only an 18% difference in the population of voxels allowed to enter the BMD computation. In subjects without SCI, the threshold peel method allowed 75% of the ROI voxels to enter the BMD analysis. Peeling the image down to 45% of the ROI yields a 30% difference in voxel population from the threshold peel method. BMD is computed as a mean value for the area accepted to enter analysis; thus, if the accepted area differs a great deal between peel methods, the BMD will also differ widely. Because voxel allocation differed by such a degree for the SCI group, BMD output differed considerably between the two peel strategies.

In order to separately analyze cortical and trabecular bone with pQCT, the image must be partitioned with either a threshold-based or a percentage-based peel. The quality of a threshold-based peel depends upon the appropriateness of the selected threshold for the bone region under scrutiny. Hangartner and colleagues recently reported guidelines for threshold selection during analysis of diaphyseal cortical bone [31]. They suggested that appropriate thresholds for delineating tissue margins can be selected according to a percentage of the density difference between the two tissues requiring partition (cortical bone and soft tissue, for example). This concept has clear merit for the analysis of cortical bone because its density does not diminish considerably after SCI [1,3]. This approach may be less useful for the analysis of rapidly changing trabecular bone regions after SCI. Different thresholds may be required for images obtained across time post-SCI, an untenable situation for longitudinal research. Unfortunately, no widely accepted guidelines yet exist for BMD thresholds in the post-SCI distal femur [1]. At the present time, investigators most commonly use visual inspection to determine the

appropriateness of endosteal thresholds in post-SCI bone. In our visual inspections of peeled images, a threshold of 400 mg/cm^3 adequately peels away cortical and subcortical voxels without eliminating peripheral trabecular voxels from the analysis. Adding a filter step aids the determination of subcortical voxels hidden among trabecular area. We have found that this threshold functions acceptably for subjects with acute or chronic SCI, making it suitable for longitudinal BMD studies.

When comparing subjects with and without SCI, investigators should carefully consider whether uniform voxel allocation would be desirable between groups. If investigators desire to compare similar bone regions between subject cohorts, using a 45% peel method would be advisable. Because trabecular degradation may preferentially occur in the center of the bone cross-section, a 45% peel may offer greater sensitivity or more rapid detection of post-SCI bone loss. Likewise, a 45% peel may allow more rapid detection of bone adaptations to unilaterally administered anti-osteoporosis interventions [32–35].

Investigators should also consider whether there may be merit to analyzing as much of the trabecular envelope as possible in subjects with SCI. We have recently demonstrated that mechanical loading via soleus muscle stimulation may induce asymmetric preservation of trabecular bone within the distal tibia cross-section [35]. Concentrically peeling away voxels with no consideration of BMD may undermine researchers' ability to detect asymmetric adaptations. Similarly, a concentric peel approach may not be appropriate for metaphyseal sites where the marrow space is large, as few trabecular voxels may be present within the central 45% of the image. A 45% concentric peel method may instead be more appropriate for epiphyseal sites with a relatively uniform distribution of trabeculae.

Finally, among subjects with SCI we observed that BMD differences among peel methods were particularly high in low-density images (Fig. 4). The analysis of images collected from subjects with chronic SCI (and thus the lowest BMD) is therefore likely to be particularly affected by the investigator's choice of peel method. In subjects with long-term SCI, using a 45% peel may result in underestimation of BMD. By the same token, using a threshold-based peel may result in overestimation of BMD. If separate analysis of the trabecular envelope is desirable, then researchers must consider which voxel allocation strategy is most advantageous for their research goals. In longitudinal studies or in studies that include a cohort of individuals with chronic SCI, this decision is of particular importance. This argues for careful consideration of peel methods at the outset of longitudinal investigations.

Effect of SCI

Although a method exists to measure distal femur BMD via conventional clinical densitometry (dual energy X-ray absorptiometry, DXA) [36], DXA cannot separately examine cortical and trabecular bone adaptations. This shortcoming obscures the extensive trabecular compartment adaptations known to occur after SCI [2,15,32]. pQCT appears to be a more suitable imaging technique for examining post-SCI BMD changes, but it is a relatively new technology undergoing continued refinement of analysis methods [31]. The relative novelty of pQCT is one reason why normative SCI and control BMD values have not yet been published for the femur metaphysis, despite its clinical significance.

BMD for the control cohort was 213.7 mg/cm^3 , which is somewhat lower than non-SCI BMD values previously reported for the tibia distal epiphysis ($\sim 250 \text{ mg/cm}^3$) [1,15]. The emergence of the marrow cavity at the femur metaphysis (but not at the tibia epiphysis -4% site) probably explains this difference. Metaphyseal slices may normally include a higher proportion of marrow voxels than epiphyseal slices.

By 8 months post-SCI (bin 2), SCI BMD values were significantly lower than non-SCI values ($p < 0.05$), supporting our first hypothesis. BMD declined precipitously in subjects with recent SCI, such that after 1.5 years, all BMD values were >1 standard deviation below the control value. Beyond 2 years, nearly all SCI BMD values fell below the lowest range of the control values (>2 SD lower). In the first 2 years after SCI, subjects lost an average of 1.7% of the projected initial BMD per month. This rate of decline is commensurate with previous estimates for other anatomic sites (2–4% per month: [7,8,37]).

In contrast, four subjects who were followed longitudinally starting ~ 2 years post-SCI demonstrated no BMD decline over time. The small sample of longitudinal data in this study prevents us from fully characterizing longitudinal BMD decline of the femur metaphysis. However, the results are congruent with a previous large cross-sectional study that characterized rapid femur epiphysis BMD decline for 3–4 years, followed by a steady state plateau thereafter [1]. No previous study has put forward a steady state BMD value for the femur metaphysis, although one report provided bone mineral content [14]. However, the BMD values demonstrated by chronic (>2 yrs) SCI subjects in the present study (~ 70 – 100 mg/cm³) are similar to previously published values for the femur epiphysis (~ 113 mg/cm³) [1]. The higher steady state value for the epiphysis (4% of femur length) in that report is congruent with our finding that trabecular BMD declines from distal to proximal in the femur. Bin 6 BMD in the present study was just 39.5% of the non-SCI BMD, a similar long-term magnitude of loss as previously reported for the distal tibia (44.8% of non-SCI BMD) [15].

Conclusions

Establishing the longitudinal effect of SCI on BMD of the femur metaphysis is an important preliminary step toward quantifying the effectiveness of novel strategies to prevent osteoporosis at this vulnerable site. In the present report, the femur metaphysis demonstrated a rapid loss of BMD followed by a relatively steady state plateau at less than 40% of non-SCI BMD. BMD differences due to 3 mm intentional slice misplacement were $\sim 2.5\%$ in subjects with and without SCI, roughly half the difference previously observed at the distal tibia epiphysis. Peel method appears to influence BMD to a greater degree than slice position in subjects with SCI (average BMD difference between a threshold-based peel and a 45% peel was 17.3% in this cohort). We feel that percentage peel methods are appropriate when special sensitivity is required to detect BMD adaptations in the center of the bone cross-section. In other experimental situations, particularly in subjects with few central trabeculae (chronic SCI) or at metaphyseal sites, a threshold-based peel method may be more advantageous. A comprehensive understanding of the sources of error in pQCT assessment will enhance future BMD studies.

Acknowledgments

The authors thank Deanna Frei, RTR, CT, and April Miller, RTR for their expertise during pQCT measurements. The authors thank Daniel Schiferl and Christopher Gordon, Ph.D. for support with pQCT technical matters. This work was supported by an award from the National Institutes of Health (R01-NR 010285-05; RKS). SDJ received a scholarship from the Foundation for Physical Therapy, Inc.

References

1. Eser P, Frotzler A, Zehnder Y, Wick L, Knecht H, Denoth J, Schiessl H. Relationship between the duration of paralysis and bone structure: a pQCT study of spinal cord injured individuals. *Bone* 2004;34:869–880. [PubMed: 15121019]
2. Modlesky CM, Majumdar S, Narasimhan A, Dudley GA. Trabecular bone microarchitecture is deteriorated in men with spinal cord injury. *J Bone Miner Res* 2004;19:48–55. [PubMed: 14753736]

3. Frey-Rindova P, de Bruin ED, Stussi E, Dambacher MA, Dietz V. Bone mineral density in upper and lower extremities during 12 months after spinal cord injury measured by peripheral quantitative computed tomography. *Spinal Cord* 2000;38:26–32. [PubMed: 10762194]
4. Modlesky CM, Slade JM, Bickel CS, Meyer RA, Dudley GA. Deteriorated geometric structure and strength of the midfemur in men with complete spinal cord injury. *Bone* 2005;36:331–339. [PubMed: 15780960]
5. Vestergaard P, Krogh K, Rejnmark L, Mosekilde L. Fracture rates and risk factors for fractures in patients with spinal cord injury. *Spinal Cord* 1998;36:790–796. [PubMed: 9848488]
6. Krause JS, Carter RE, Pickelsimer EE, Wilson D. A prospective study of health and risk of mortality after spinal cord injury. *Arch Phys Med Rehabil* 2008;89:1482–1491. [PubMed: 18674984]
7. Garland DE, Stewart CA, Adkins RH, Hu SS, Rosen C, Liotta FJ, Weinstein DA. Osteoporosis after spinal cord injury. *J Orthop Res* 1992;10:371–378. [PubMed: 1569500]
8. Wilmet E, Ismail AA, Heilporn A, Welraeds D, Bergmann P. Longitudinal study of the bone mineral content and of soft tissue composition after spinal cord section. *Paraplegia* 1995;33:674–677. [PubMed: 8584304]
9. Frotzler A, Coupaud S, Perret C, Kakebeeke TH, Hunt KJ, Eser P. Effect of detraining on bone and muscle tissue in subjects with chronic spinal cord injury after a period of electrically-stimulated cycling: a small cohort study. *J Rehabil Med* 2009;41:282–285. [PubMed: 19247550]
10. Frotzler A, Berger M, Knecht H, Eser P. Bone steady-state is established at reduced bone strength after spinal cord injury: a longitudinal study using peripheral quantitative computed tomography (pQCT). *Bone* 2008;43(3):549–555. [PubMed: 18567554]
11. Keating JF, Kerr M, Delargy M. Minimal trauma causing fractures in patients with spinal cord injury. *Disabil Rehabil* 1992;14:108–109. [PubMed: 1600181]
12. Garland DE, Adkins RH. Bone loss at the knee in spinal cord injury. *Top Spinal Cord Inj Rehabil* 2001;6:37–46.
13. Comarr AE, Hutchinson RH, Bors E. Extremity fractures of patients with spinal cord injuries. *Am J Surg* 1962;103:732–739. [PubMed: 13880733]
14. Rittweger J, Gerrits K, Altenburg T, Reeves N, Maganaris CN, de Haan A. Bone adaptation to altered loading after spinal cord injury: a study of bone and muscle strength. *J Musculoskelet Neuronal Interact* 2006;6:269–276. [PubMed: 17142949]
15. Shields RK, Dudley-Javoroski S, Boaldin KM, Corey TA, Fog DB, Ruen JM. Peripheral quantitative computed tomography: measurement sensitivity in persons with and without spinal cord injury. *Arch Phys Med Rehabil* 2006;87:1376–1381. [PubMed: 17023249]
16. Eser P, Frotzler A, Zehnder Y, Denoth J. Fracture threshold in the femur and tibia of people with spinal cord injury as determined by peripheral quantitative computed tomography. *Arch Phys Med Rehabil* 2005;86:498–504. [PubMed: 15759235]
17. American Spinal Injury Association. International Standards for Neurological Classification of SCI. American Spinal Injury Association; Atlanta: 2002.
18. Ben M, Harvey L, Denis S, Glinsky J, Goehl G, Chee S, Herbert RD. Does 12 weeks of regular standing prevent loss of ankle mobility and bone mineral density in people with recent spinal cord injuries? *Aust J Physiother* 2005;51:251–256. [PubMed: 16321132]
19. Kunkel CF, Scremin AM, Eisenberg B, Garcia JF, Roberts S, Martinez S. Effect of “standing” on spasticity, contracture, and osteoporosis in paralyzed males. *Arch Phys Med Rehabil* 1993;74:73–78. [PubMed: 8420525]
20. Norland Medical Systems I. XCT 2000 Technical Reference. Norland Medical Systems, Inc; White Plains: 2000.
21. Portney, LG.; Watkins, MP. Foundations of clinical research: applications to practice. Pearson Education, Inc; Upper Saddle River: 2009.
22. Hangartner TN, Gilsanz V. Evaluation of cortical bone by computed tomography. *J Bone Miner Res* 1996;11:1518–1525. [PubMed: 8889852]
23. Eser P, Frotzler A, Zehnder Y, Schiessl H, Denoth J. Assessment of anthropometric, systemic, and lifestyle factors influencing bone status in the legs of spinal cord injured individuals. *Osteoporos Int* 2005;16:26–34. [PubMed: 15138665]

24. Frotzler A, Coupaud S, Perret C, Kakebeeke TH, Hunt KJ, Donaldson Nde N, Eser P. High-volume FES-cycling partially reverses bone loss in people with chronic spinal cord injury. *Bone* 2008;43:169–176. [PubMed: 18440891]
25. Eser P, Schiessl H, Willnecker J. Bone loss and steady state after spinal cord injury: a cross-sectional study using pQCT. *J Musculoskelet Neuronal Interact* 2004;4:197–198. [PubMed: 15615125]
26. Rauch F, Tuttlewski B, Fricke O, Rieger-Wettengl G, Schauseil-Zipf U, Herkenrath P, Neu CM, Schoenau E. Analysis of cancellous bone turnover by multiple slice analysis at distal radius: a study using peripheral quantitative computed tomography. *J Clin Densitom* 2001;4:257–262. [PubMed: 11791503]
27. Lee DC, Gilsanz V, Wren TA. Limitations of peripheral quantitative computed tomography metaphyseal bone density measurements. *J Clin Endocrinol Metab* 2007;92:4248–4253. [PubMed: 17684050]
28. Holliday TW, Ruff CB. Relative variation in human proximal and distal limb segment lengths. *Am J Phys Anthropol* 2001;116:26–33. [PubMed: 11536114]
29. Shultz SJ, Nguyen AD. Bilateral asymmetries in clinical measures of lower-extremity anatomic characteristics. *Clin J Sport Med* 2007;17:357–361. [PubMed: 17873547]
30. Jantz LM, Jantz RL. Secular change in long bone length and proportion in the United States, 1800–1970. *Am J Phys Anthropol* 1999;110:57–67. [PubMed: 10490468]
31. Hangartner TN. Thresholding technique for accurate analysis of density and geometry in QCT, pQCT and muCT images. *J Musculoskelet Neuronal Interact* 2007;7:9–16. [PubMed: 17396001]
32. Shields RK, Dudley-Javoroski S. Musculoskeletal plasticity after acute spinal cord injury: effects of long-term neuromuscular electrical stimulation training. *J Neurophysiol* 2006;95:2380–2390. [PubMed: 16407424]
33. Shields RK, Dudley-Javoroski S. Musculoskeletal adaptation in chronic spinal cord injury: effects of long-term soleus electrical stimulation training. *J Neurorehab and Neural Re* 2006;21:169–179.
34. Dudley-Javoroski S, Shields RK. Dose estimation and surveillance of mechanical loading interventions for bone loss after spinal cord injury. *Phys Ther* 2008;88:387–396. [PubMed: 18202080]
35. Dudley-Javoroski S, Shields RK. Asymmetric bone adaptations to soleus mechanical loading after spinal cord injury. *J Musculoskelet Neuronal Interact* 2008;8:227–238. [PubMed: 18799855]
36. Shields RK, Schlechte J, Dudley-Javoroski S, Zwart BD, Clark SD, Grant SA, Mattiace VM. Bone mineral density after spinal cord injury: a reliable method for knee measurement. *Arch Phys Med Rehabil* 2005;86:1969–1973. [PubMed: 16213240]
37. Biering-Sorensen F, Bohr HH, Schaadt OP. Longitudinal study of bone mineral content in the lumbar spine, the forearm and the lower extremities after spinal cord injury. *Eur J Clin Invest* 1990;20:330–335. [PubMed: 2114994]

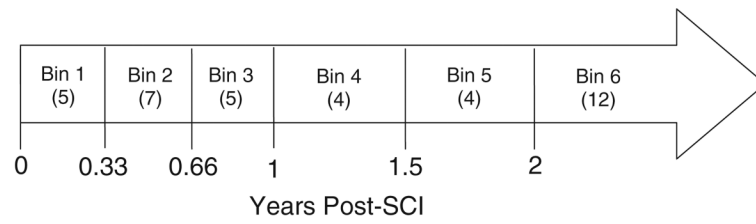


Fig. 1. Time bins used to partition longitudinal data. *Boldface numerals* represent the time post-SCI (years) at the end of each time bin. *Numerals in parentheses* indicate the number of data points included in each time bin

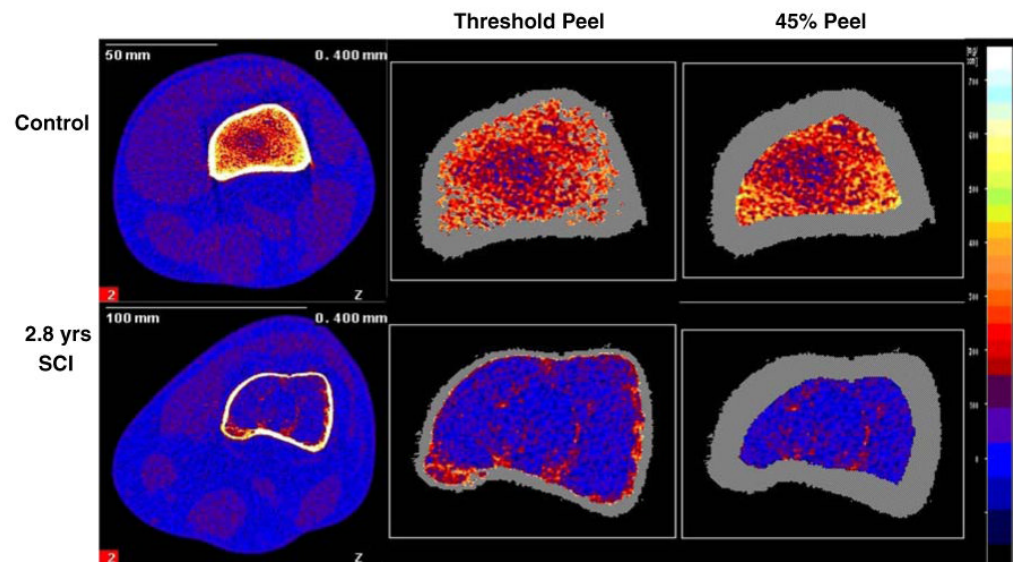


Fig. 2. Representative examples of pQCT images at the femur metaphysis for subjects with and without SCI. Images are normalized to fat density, represented as *bright blue* on the color scale. *Orange and red voxels* correspond to trabecular bone and *yellow and white voxels* correspond to subcortical and cortical bone. The leftmost image for each subject was captured at the 12% femur metaphysis site. The two rightmost images for each subject demonstrate the “threshold peel” and 45% peel voxel allocation strategies

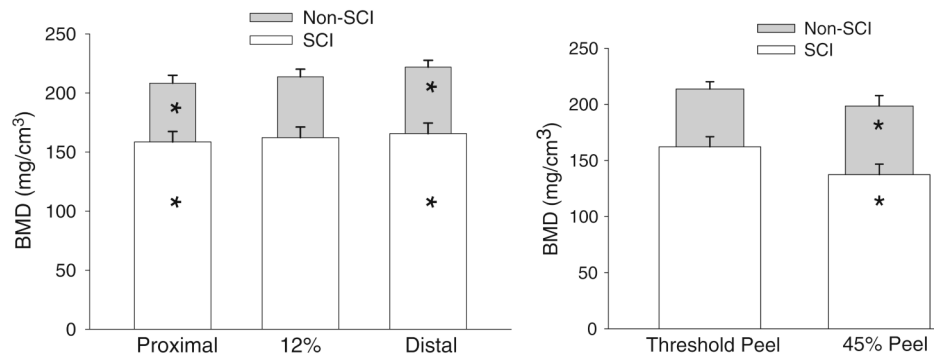


Fig. 3.

Left: effect of slice placement. All BMD values were obtained using the “threshold peel” voxel allocation method. Mean (SE) BMD values (mg/cm³) for the three slice locations for subjects with and without SCI. *—different from the corresponding 12% slice ($p < 0.05$). Right: effect of peel method. Mean (SE) BMD values (mg/cm³) for the 12% slice location with two different peel methods. *—different from the corresponding “threshold peel” condition ($p < 0.05$)

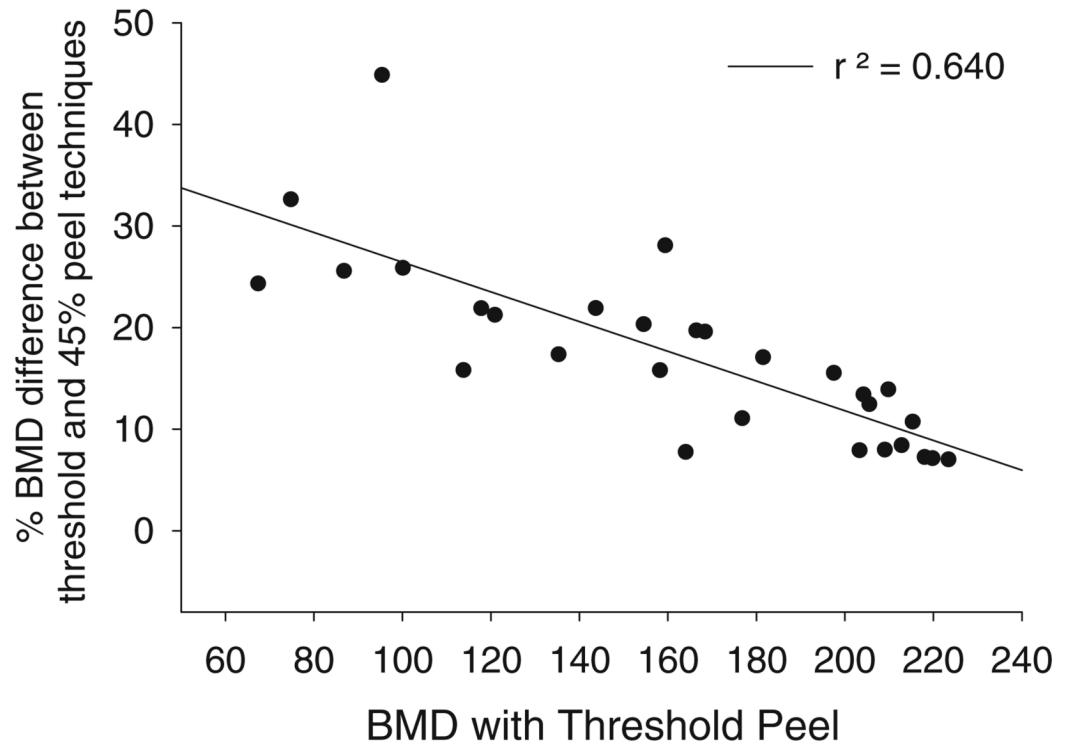


Fig. 4. Relationship between threshold peel-based BMD and the percent difference in BMD obtained between the threshold peel and the 45% peel methods. BMD differences due to processing methods are most pronounced in images with low BMD

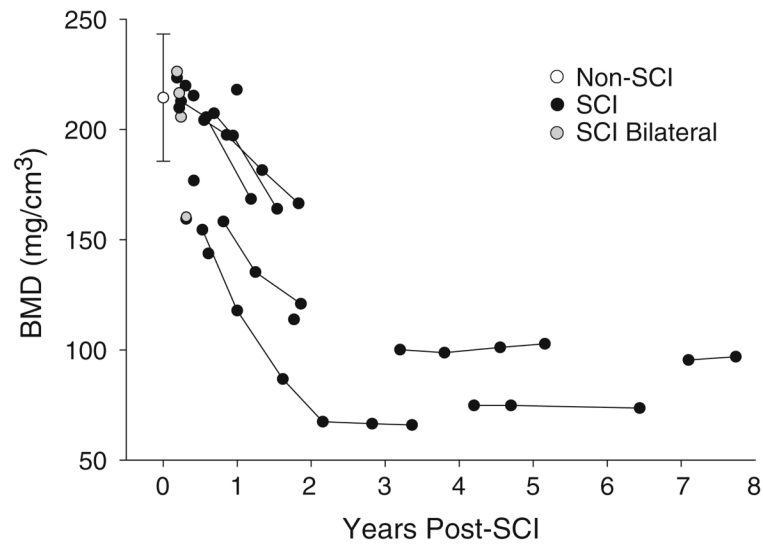


Fig. 5. Trabecular BMD of the 12% femur metaphysis site, using the “threshold peel” voxel allocation method. Non-SCI plot is mean/SD. Five SCI subjects were initially tested within 0.33 years post-SCI (bin 1); four of these subjects underwent bilateral scans, which appear as *gray plots*. *Data points joined by lines* represent limbs that were sampled longitudinally

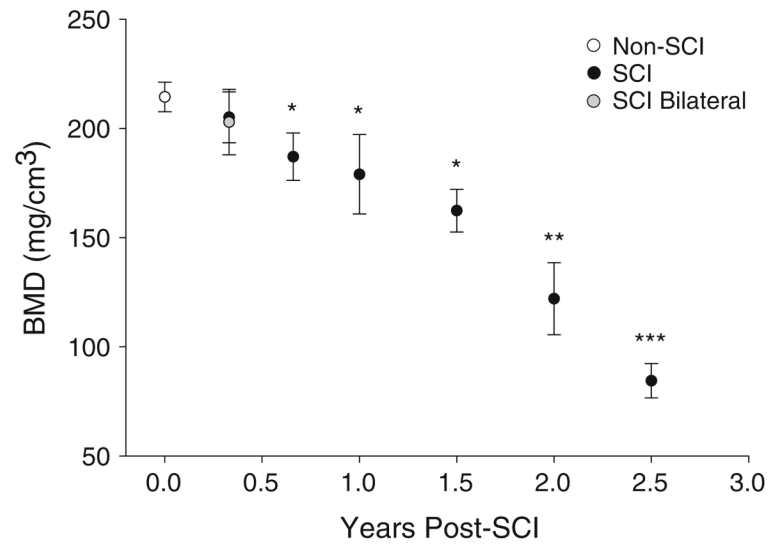


Fig. 6.

Data (threshold peel analysis method) were partitioned into time bins (Fig. 1) so that the maximum data points were included from the longitudinal data set (Fig. 5), but no subject appeared more than once in any bin. Data are mean/SE BMD for each time bin, shown at the corresponding time post-SCI on the x -axis. * = different from the non-SCI value ($p < 0.05$). ** = different from non-SCI, bin 1 and bin 2. *** = different from non-SCI and bins 1–4

Table 1

Subject demographic data

Subject number	Sex	Age at SCI	Age at first pQCT	SCI years at first pQCT	SCI level	ASIA grade	Left femur length	Right femur length	Samples	Bins
S1	M	18	18	0.19	T11	A	440	435	3	1, 2
S2	M	37	37	0.22	T10	A	452	458	2	1
S3	M	20	20	0.24	T8	A	525	495	4	1, 2, 4
S4	M	28	28	0.30	T7	A	512	510	5	2-5
S5	M	49	49	0.31	C7	B	468	455	2	1
S6	F	18	18	0.41	T8	A	383	382	1	2
S7	M	38	38	0.53	T8	A	515	510	6	2, 3, 5, 6
S8	M	43	44	0.61	T4	A	446	446	1	2
S9	M	33	34	0.68	T11	B	435	435	3	2-4
S10	M	22	22	0.81	T11	A	415	410	3	3-5
S11	M	25	26	0.99	T10	A	455	437	1	3
S12	M	32	34	1.77	T6	A	510	509	1	5
S13	M	21	24	3.20	T4	A	481	N/A	4	6
S14	M	22	26	4.20	T4	A	480	N/A	3	6
S15	M	29	36	7.10	T9	A	475	N/A	2	6
SCI mean	-	-	30	-	-	-	466	457	-	-
N1	M	-	23	-	-	-	489	485	2	-
N2	M	-	24	-	-	-	484	485	2	-
N3	M	-	42	-	-	-	471	472	2	-
N4	F	-	22	-	-	-	445	437	2	-
N5	M	-	30	-	-	-	454	482	2	-
N6	M	-	26	-	-	-	486	472	2	-
N7	M	-	24	-	-	-	466	469	1	-
N8	M	-	24	-	-	-	480	472	2	-
N9	M	-	24	-	-	-	476	475	2	-
N10	M	-	34	-	-	-	525	530	2	-
Control mean	-	-	27	-	-	-	478	478	-	-

“S” denotes subjects in the SCI cohort, and “N” denotes non-SCI control subjects. Subject cohorts did not differ according to age ($p=0.75$) or left femur length ($p=0.42$). Femur length is given in mm. “Samples” refers to the number of data points each subject contributed to Fig. 5, via bilateral and/or longitudinal assessment.